



中央研究院
資訊科學研究所

Institute of Information Science, Academia Sinica • Taipei, Taiwan, ROC

TR-IIS-23-001

Turning with Curvature Constraint: G^3

Trajectory Solution Using Seventh

Degree B'ezier Curves Design

Ting-Wei Hsu , Jing-Sin Liu



Jan. 6, 2023

||

Technical Report No. TR-IIS-23-001

<https://www.iis.sinica.edu.tw/zh/page/Library/TechReport/2023.html>

Turning with Curvature Constraint: G^3 Trajectory Solution Using Seventh Degree Bézier Curves Design

Ting-Wei Hsu¹, Jing-Sin Liu²

¹Department of Mechanical Engineering, National Taiwan University, Taipei, Taiwan

²Institute of Information Science, Academia Sinica, Taipei, Taiwan

Abstract

Curvature constraint is an essential constraint for smooth turning because of the physical limitation of vehicles on lateral acceleration during turning. In this research, we present three practical curvature-constrained smooth turning scenarios for autonomous vehicle maneuvering scenarios: ordinary turn, lane change on straight road, and lane change in roundabout. For each scenario, instead of using concatenated path segments of lower-order curves, like cubic Bézier curves, we use the equivalent 7th-degree Bézier curves of simplified η^3 -splines to design smooth uni-directional turning paths. The scenarios serve well to illustrate that various curvature-constrained turning paths of 7th-degree Bézier form can be generated successfully through flexible selections of suitable parameter values by the user or an iterative-search-and-verify process to explore the feasible parameter set in a more intuitive and computationally simpler manner. Mathematical inductions and examples are given in each scenario, and the plots of the relationship between maximum curvature and the assigned parameter show how our methods work.

Keywords— Bézier Curve, η^3 -spline, Curvature Constraints, Autonomous Driving, Path planning

1 Introduction

Safety benefits expected by the automated driving systems are supported by fast and efficient online trajectory planning. A simple smooth trajectory generation method is therefore a desirable feature. To attain efficiency and flexibility of path planning, the a priori chosen path primitives that meet boundary conditions and smoothness requirements can be employed to allow easy adaptation to complex environments and unexpected events.

These requirements therefore constitute certain type of path planning problem where curvature constraint is more important to be taken into account. Though, there are various algorithms and types of path primitives that take curvature profile into consideration, however, some of them are not kinematically feasible like visibility graphs. For problems with tougher requirements such as lane change between two parallel lanes or within roundabout, curvature affects directly the shape of the path, allowable velocity and normal acceleration, and lets the velocity should be slower on path segments with larger curvature than with small curvature. Therefore, an appropriate path for tracking and control should be considered with smaller variation of curvature. For generating smooth, kinematically feasible and safe trajectory which is taken by the vehicle on the road with as low computation (fast) as possible, we demand it by real-time safe operation of practical scenarios such as autonomous vehicles, and urban driving in complex section of the route. With these conditions, spline interpolation is often a preferred option of parametrized polynomial trajectory primitives since the boundary conditions and smoothness that are consistent with the vehicle dynamics are encoded in the splines. Since G^2 continuous paths can result in jerky vehicle motion, to ensure driving comfort, G^3 continuity of the path to be followed by the vehicle is required. With all these conditions met above, curves, with curve parametrization ranging from splines, to cubic or quintic polynomials, to cubic spirals, and clothoids are popular to applications to perform the trajectory generation.

Trajectories based on parametrized polynomials with the closed-form path representation can shorten the planning time and need very little memory to meet real-time requirements. The reason is that the derivatives of parametric polynomials are also polynomials whose coefficients depend linearly on the coefficients of the trajectory so that the trajectory generation based on parametric polynomials can be reduced to the determination or optimization of finite parameters to enhance the performance.

Among the parametric polynomial curves used in practical scenarios such as urban driving, Bézier curves are one of the most well-known, popular, and extensively used parametric curves which have pleasant properties such as smoothness and convex hull. Since in complex section of the route, the trajectory is required to be light and fast computing, the Bézier curve which is based on polynomials and interpolated by its control points thus requires low computation time and very little memory for real-time trajectory generation and is the best choice. By enforcing the convex hull of the chosen control points not intersect obstacles, the Bézier path constructed from

the control points will be inside the convex hull and therefore collision-free. The smoothness of Bézier curves guarantees that the path equation is continuous, including its first and second-order derivatives. Therefore, we can just easily assign the control points to generate a smooth curve. In trajectory planning, some papers use Bézier curves to design the path in the scenario of lane change [1][2][3] and in roundabout path planning [4][5]. Path planning algorithms, like RRT, use Bézier curves to smooth the jagged path [6][7][8]. However, the curvature and curvature derivative of Bézier curves are nonlinear functions of control points and their derivatives. It is hard to design high-order Bézier curves complying with curvature and curvature derivative constraints.

Note, depending on the smoothness requirement, trajectory generation with curve parametrization (path primitives) using different types of curves, ranging from splines, to cubic, quartic, quintic polynomials, to curvature-defining curves such as clothoids and cubic spirals, are proposed. To attain efficiency and flexibility of path or trajectory planning, the a priori chosen path primitives that meet boundary conditions and smoothness requirements are particularly useful. For further path computational efficiency, it is desirable to reduce the DoFs of a path primitive whenever possible. A common approach to trajectory planning is polynomial due to its design simplicity. Trajectory based on polynomials needs low computation time and very little memory, thus suited well for real-time applications. However, high order (more than 5) polynomial also has more coefficients to be determined, and complicated curvature expression, thus more computationally expensive. It has not yet been extensively studied in trajectory planning with some exceptions [16][8].

For smoothing sharp corner, curvature-continuous and bounded curvature path is generated based on concatenation of two cubic degree Bézier curves [22]. Quartic Bézier curve was proposed to generate a G^2 (continuous-curvature) trajectory with curvature and velocity constraints [17]. Only 3 free parameters are required to determine the 5 control points defining the quartic Bézier curve.

A continuous-curvature curvature-constrained path computed by CC-steer is composed by tangential line segments, circular arcs and clothoid arcs with closed-form curvature expression [18]. However, lack of closed-form path expression of cc-steer makes the path computation and following can be achieved only approximately. A single interpolating polynomial path, called η^3 -spline, was proposed for a path with continuous-curvature derivative [18].

A flexible approach was the concatenation of multiple path segments, which may be different, connected with smoothness requirement. Bi-elementary path based on clothoid in combination with arc was proposed for lane change on curved road with small curvature [19]. This leads to additional computational effort for joining the different segments. This work [20] proposed a cubic B-spline based continuous curvature (G^2) curvature-constrained forward-backward path generation method, with small curvature derivative discontinuity.

Piazzini et al.[9] invented a kind of 7^{th} -order curve called η^3 -splines. η^3 -splines help us design paths easily as we only need to assign the boundary conditions, i.e. the position, direction, curvature, and derivative of curvature of endpoints and a vector called η vector which contains 6 path-defining parameters to adjust the path. Since the configurability of the curve is very flexible but results in a huge search space and causes unacceptable executing time, we can reduce the DOFs to 2 to save the computation time. η^3 -splines of that kind are called simplified η^3 -splines. In our previous research[10], we found the relation between simplified η^3 -splines and 7^{th} -order Bézier curves. With this relation, simplified η^3 -splines can be transformed into Bézier curves. As a result, a simplified η^3 -spline can be seen as a curve that combines both the benefits of η^3 -splines and Bézier curves, i.e. the simplicity of design from η^3 -splines and the collision-free detection method by finding convex hull from Bézier curves. We also presented some applications for the conversion method in our previous works[10][11].

In the practical aspect, curves need to fulfill the physical limits of vehicles, such as velocity, acceleration, and curvature limit. Many authors discuss how to constraint curvature with all kinds of curves. Choi et al. [12] gave the explicit solution for maximum curvature of a 3^{rd} -order Bézier curve. Cimurs et al. [13] assigned a circle with the minimum radius and made the curve fit the circle by adjusting control points of a 3^{rd} -order Bézier curve. Li et al.[14] set up a multi-objective function to consider the boundary conditions including maximum curvature for a 5^{th} -order Bézier curve.

The higher the order is, the more we can control the curve by adding more boundary constraints, such as curvature and derivative of curvature of endpoints. For example, the derivative of curvature at the endpoints in a 5^{th} -order Bézier curve cannot be 0, but a 7^{th} -order Bézier curve can. However, high-order polynomial functions have more coefficients to be determined and thus cause complicated curvature expression. Most papers focus on implementing 7^{th} -order Bézier curves instead of discussing how to constraint maximum curvature. For example, Neto et al.[8] used 7^{th} -order Bézier curves to let the endpoints curvature be 0 so that it is simpler to implement RRT algorithm.

To account for arbitrary nonzero curvature and arbitrary curvature derivative at either one or both ends of the curve such as entering the roundabout or curved road, our previous work [10] proposed a transformation that brings a family of 2-parameter η^3 -splines into equivalent 7^{th} -degree Bézier curves as the simplest single directional smooth maneuver from the start to the goal. In this paper, focusing specifically on turning on the road in a wide range of driving scenarios, lane change in particular, a forward uni-directional trajectory based on simplified η^3 -splines, which have flexibility to take safety and comfort (limited lateral acceleration or curvature) into account, is generated. A feasible trajectory can be found by iteratively searching the trajectory parameters η_1 and η_2 of simplified η^3 -splines for determining the control points of its natural equivalent 7^{th} -degree Bézier curve and trajectory duration T until all obstacles are avoided in the environment, while curvature

constraints are not violated and other kinodynamic requirements are met. These results can be applied in many applications and autonomous driving for example as a G^3 continuity solution to specific curvature constrained turning maneuver problems is required. The convenience of this computationally simpler approach can be extended to multiple maneuvers, for example to steer the tractor-trailer [10]. The determination of the number and location of waypoints for multiple maneuvers based on simplified η^3 splines, is proposed a variable length genetic algorithm in combination with bidirectional RRT^* in our early work [15].

The main contributions in this research are listed as the followings.

1. We discuss how to constrain curvature on 7^{th} -order Bézier curves instead of lower-order curves. The restriction of zero curvature at both ends of the path such as required in driving on straight roads is alleviated by the use of 7th degree Bézier curve for driving on curved roads.
2. We solve the curvature constraint problem case by case since it is hard to get the general form of curvature equation for 7^{th} -order Bézier curves.
3. we discover the simplicity and flexibility of path design which relies on only two parameters at most for planning the control points intuitively and iteratively.
4. We provide other numerical simulation data for designed paths of 7^{th} -order Bézier curves by considering maximum curvature.

And the benefits of our path design can be organized as below.

1. A dynamically feasible trajectory is a trajectory complying with the constraints (boundary conditions, kinodynamic constraints etc.). The feasibility set is representative of the dynamic as well as operational constraints for checking the validity of kinematic geometric path. The feasible space of the path-defining parameters of a simplified η^3 -spline is reduced to a box (a parametric interval for each parameter), allowing path optimization treated as easier parameter optimization with computational efficiency for online path generation.
2. Since G^3 continuity (third-order geometric continuity) ensures continuous jerk, while G^2 doesn't. It allows path optimization of the paths with respect to a cost function such as jerk or consumed energy to minimize the curvature derivative.
3. An advantage of using the 7^{th} degree Bézier form is we can generate various paths through selection of suitable parameter values in a more intuitive manner. Specifying nonzero boundary curvature and incorporating collision avoidance at the same time can be achieved more easily and intuitively to some extent via the Bézier form, and its closed-form provides a low complexity of trajectory computation. Therefore, we will use the Bézier form of simplified η^3 spline to simplify the manipulation of the curve by manipulating the convex hull confining the spatial extent of the curve: If the convex hull for the chosen control points doesn't intersect the obstacles, then the Bézier path constructed from the control points will be collision-free.

The rest of this paper is organized as the following. Section 2 gives a brief introduction of Bézier curve, η^3 -spline, and the relation between Bézier curve and η^3 -spline. Section 3 illustrates the design method in three road scenarios with examples. Section 4 gives the conclusion and future work.

2 Bézier curve and η^3 -spline

2.1 Bézier Curve

Bézier Curves are curves using control points to shape outlines as shown in FIGURE 1. To implement, we have to assign $n + 1$ control points P_0, P_1, \dots, P_n to interpolate curves with Bernstein polynomial functions. The curve function is shown in (1).

$$C(t) = \sum_{i=0}^n B_{i,n}(t)P_i \quad (1)$$

$B_{i,n}(t)$ in (1) is Bernstein polynomials. The definition is defined as (2) and (3),

$$B_{i,n} = \binom{n}{i} t^i (1-t)^{n-i}, i = 0, 1, \dots, n, \quad (2)$$

$$\binom{n}{i} = \frac{n!}{i!(n-i)!} \quad (3)$$

The term n in (1), (2), and (3) is the order of Bézier curve. For an n^{th} order Bézier curve, $n + 1$ control points are needed. The parameter t , ranging from 0 to 1, is the input domain of Bernstein polynomial functions.

A pleasant property of Bézier curve is that the curve lies inside the convex hull, which means curves would never stretch over the edges of the smallest convex polygon formed by control points. When $t = 0$ or $t = 1$, the result of (1) is P_0 or P_n respectively. Therefore, the first and the last control points of a Bézier curve are coincident with end points respectively. FIGURE 1 shows an example of Bézier curve and its convex hull.

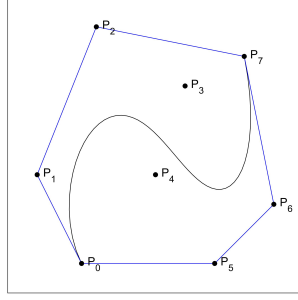


Figure 1: A 7th-order Bézier curve with control points P_0 to P_7 . The convex hull of the control points is shown as the polygon with blue edges. [10]

2.2 η^3 -spline

An η^3 -spline is a 7th order curve with given boundary conditions to define it[9]. The boundary conditions are

$$\Omega_A = [x_A, y_A, \theta_A, \kappa_A, \dot{\kappa}_A]^T, \quad (4)$$

and

$$\Omega_B = [x_B, y_B, \theta_B, \kappa_B, \dot{\kappa}_B]^T, \quad (5)$$

where x and y are the Cartesian coordinates, and θ , κ and $\dot{\kappa}$ respectively denotes the direction that defines the unit tangent along the curve $[\cos \theta, \sin \theta]$, curvature and derivative of curvature of the given point.

The equation of an η^3 -spline is defined as the following:

$$C(t) = [\alpha(t) \beta(t)]^T \quad (6)$$

$$\alpha(t) = \alpha_0 + \alpha_1 t + \alpha_2 t^2 + \alpha_3 t^3 + \alpha_4 t^4 + \alpha_5 t^5 + \alpha_6 t^6 + \alpha_7 t^7 \quad (7)$$

$$\beta(t) = \beta_0 + \beta_1 t + \beta_2 t^2 + \beta_3 t^3 + \beta_4 t^4 + \beta_5 t^5 + \beta_6 t^6 + \beta_7 t^7 \quad (8)$$

where t is the same variable that defines Bézier curve, ranging from 0 to 1. The coefficients α_i and β_i for $i = 0, 1, \dots, 7$ in (7) and (8) are defined as

$$\alpha_0 = x_A \quad (9)$$

$$\alpha_1 = \eta_1 \cos \theta_A \quad (10)$$

$$\alpha_2 = \frac{1}{2} \eta_3 \cos \theta_A - \frac{1}{2} \eta_1^2 \kappa_A \sin \theta_A \quad (11)$$

$$\alpha_3 = \frac{1}{6} \eta_5 \cos \theta_A - \frac{1}{6} (\eta_1^3 \dot{\kappa}_A + 3\eta_1 \eta_3 \kappa_A) \sin \theta_A \quad (12)$$

$$\begin{aligned} \alpha_4 = & 35(x_B - x_A) - (20\eta_1 + 5\eta_3 + \frac{2}{3}\eta_5) \cos \theta_A + (5\eta_1^2 \kappa_A + \frac{2}{3}\eta_1^3 \dot{\kappa}_A + 2\eta_1 \eta_3 \kappa_A) \sin \theta_A \\ & - (15\eta_2 - \frac{5}{2}\eta_4 + \frac{1}{6}\eta_6) \cos \theta_B - (\frac{5}{2}\eta_2^2 \kappa_B - \frac{1}{6}\eta_2^3 \dot{\kappa}_B - \frac{1}{2}\eta_2 \eta_4 \kappa_B) \sin \theta_B \end{aligned} \quad (13)$$

$$\begin{aligned} \alpha_5 = & -84(x_B - x_A) + (45\eta_1 + 10\eta_3 + \eta_5) \cos \theta_A - (10\eta_1^2 \kappa_A + \eta_1^3 \dot{\kappa}_A + 3\eta_1 \eta_3 \kappa_A) \sin \theta_A \\ & + (39\eta_2 - 7\eta_4 + \frac{1}{2}\eta_6) \cos \theta_B + (7\eta_2^2 \kappa_B - \frac{1}{2}\eta_2^3 \dot{\kappa}_B - \frac{3}{2}\eta_2 \eta_4 \kappa_B) \sin \theta_B \end{aligned} \quad (14)$$

$$\begin{aligned} \alpha_6 = & 70(x_B - x_A) - (36\eta_1 + \frac{15}{2}\eta_3 + \frac{2}{3}\eta_5) \cos \theta_A + (\frac{15}{2}\eta_1^2 \kappa_A + \frac{2}{3}\eta_1^3 \dot{\kappa}_A + 2\eta_1 \eta_3 \kappa_A) \sin \theta_A \\ & - (34\eta_2 - \frac{13}{2}\eta_4 + \frac{1}{2}\eta_6) \cos \theta_B - (\frac{13}{2}\eta_2^2 \kappa_B - \frac{1}{2}\eta_2^3 \dot{\kappa}_B - \frac{3}{2}\eta_2 \eta_4 \kappa_B) \sin \theta_B \end{aligned} \quad (15)$$

$$\begin{aligned} \alpha_7 = & -20(x_B - x_A) + (10\eta_1 + 2\eta_3 + \frac{1}{6}\eta_5) \cos \theta_A - (2\eta_1^2 \kappa_A + \frac{1}{6}\eta_1^3 \dot{\kappa}_A + \frac{1}{2}\eta_1 \eta_3 \kappa_A) \sin \theta_A \\ & + (10\eta_2 - 2\eta_4 + \frac{1}{6}\eta_6) \cos \theta_B + (2\eta_2^2 \kappa_B - \frac{1}{6}\eta_2^3 \dot{\kappa}_B - \frac{1}{2}\eta_2 \eta_4 \kappa_B) \sin \theta_B \end{aligned} \quad (16)$$

$$\beta_0 = y_A \quad (17)$$

$$\beta_1 = \eta_1 \sin \theta_A \quad (18)$$

$$\beta_2 = \frac{1}{2} \eta_3 \sin \theta_A + \frac{1}{2} \eta_1^2 \kappa_A \cos \theta_A \quad (19)$$

$$\beta_3 = \frac{1}{6} \eta_5 \sin \theta_A + \frac{1}{6} (\eta_1^3 \dot{\kappa}_A + 3\eta_1 \eta_3 \kappa_A) \cos \theta_A \quad (20)$$

$$\begin{aligned}\beta_4 = & 35(y_B - y_A) - (20\eta_1 + 5\eta_3 + \frac{2}{3}\eta_5) \sin \theta_A - (5\eta_1^2 \kappa_A + \frac{2}{3}\eta_1^3 \dot{\kappa}_A + 2\eta_1\eta_3\kappa_A) \cos \theta_A \\ & - (15\eta_2 - \frac{5}{2}\eta_4 + \frac{1}{6}\eta_6) \sin \theta_B + (\frac{5}{2}\eta_2^2 \kappa_B - \frac{1}{6}\eta_2^3 \dot{\kappa}_B - \frac{1}{2}\eta_2\eta_4\kappa_B) \cos \theta_B\end{aligned}\quad (21)$$

$$\begin{aligned}\beta_5 = & -84(y_B - y_A) + (45\eta_1 + 10\eta_3 + \eta_5) \sin \theta_A + (10\eta_1^2 \kappa_A + \eta_1^3 \dot{\kappa}_A + 3\eta_1\eta_3\kappa_A) \cos \theta_A \\ & + (39\eta_2 - 7\eta_4 + \frac{1}{2}\eta_6) \sin \theta_B - (7\eta_2^2 \kappa_B - \frac{1}{2}\eta_2^3 \dot{\kappa}_B - \frac{3}{2}\eta_2\eta_4\kappa_B) \cos \theta_B\end{aligned}\quad (22)$$

$$\begin{aligned}\beta_6 = & 70(y_B - y_A) - (36\eta_1 + \frac{15}{2}\eta_3 + \frac{2}{3}\eta_5) \sin \theta_A - (\frac{15}{2}\eta_1^2 \kappa_A + \frac{2}{3}\eta_1^3 \dot{\kappa}_A + 2\eta_1\eta_3\kappa_A) \cos \theta_A \\ & - (34\eta_2 - \frac{13}{2}\eta_4 + \frac{1}{2}\eta_6) \sin \theta_B + (\frac{13}{2}\eta_2^2 \kappa_B - \frac{1}{2}\eta_2^3 \dot{\kappa}_B - \frac{3}{2}\eta_2\eta_4\kappa_B) \cos \theta_B\end{aligned}\quad (23)$$

$$\begin{aligned}\beta_7 = & -20(y_B - y_A) + (10\eta_1 + 2\eta_3 + \frac{1}{6}\eta_5) \sin \theta_A + (2\eta_1^2 \kappa_A + \frac{1}{6}\eta_1^3 \dot{\kappa}_A + \frac{1}{2}\eta_1\eta_3\kappa_A) \cos \theta_A \\ & + (10\eta_2 - 2\eta_4 + \frac{1}{6}\eta_6) \sin \theta_B - (2\eta_2^2 \kappa_B - \frac{1}{6}\eta_2^3 \dot{\kappa}_B - \frac{1}{2}\eta_2\eta_4\kappa_B) \cos \theta_B\end{aligned}\quad (24)$$

The coefficients α_i in (9)-(16) and β_i in (17)-(24) for $i = 0, 1, \dots, 7$ in (7) and (8) depend on the η vector,

$$\eta = [\eta_1 \quad \eta_2 \quad \eta_3 \quad \eta_4 \quad \eta_5 \quad \eta_6]^T. \quad (25)$$

The η vector makes η^3 -spline has 6 degrees of freedom. For further path computational efficiency, it is desirable to reduce the DoFs of η^3 -spline by setting $\eta_3 = \eta_4 = \eta_5 = \eta_6 = 0$. Therefore, the degree of freedom reduces to 2, and the resulting family of parametrized curves with parameters η_1, η_2 is called simplified η^3 -spline.

Note, the lateral acceleration is restricted to account for curvature constraint. And both longitudinal and lateral accelerations can be adjusted by free parameters (control points) to uniformly accelerate from η_1 to η_2 so as to turn gently at a lower speed without a sharp spike to comply with the curvature limit. Increasing the start speed and end speed over all feasible trajectories can be effective to reduce the maneuver time (duration of the trajectory).

2.3 The conversion method between Bézier curve and η^3 -spline

As shown in [10], since simplified η^3 -spline is 7th order curve, we consider a 7th order Bézier curve. Assign n as 7, equation (1) will be

$$\begin{aligned}C(t) = & P_0(1-t)^7 + 7P_1t(1-t)^6 + 21P_2t^2(1-t)^5 + 35P_3t^3(1-t)^4 \\ & + 35P_4t^4(1-t)^3 + 21P_5t^5(1-t)^2 + 7P_6t^6(1-t) + P_7t^7\end{aligned}\quad (26)$$

P_i is a vector containing 2 components P_{xi} and P_{yi} which indicate the x and y coordinates of P_i . Expand (26) and match the coefficients of simplified η^3 -splines in (9)-(24), we find

$$P_{x0} = x_A \quad (27)$$

$$P_{x1} = x_A + \frac{1}{7}\eta_1 \cos \theta_A \quad (28)$$

$$P_{x2} = x_A + \frac{2}{7}\eta_1 \cos \theta_A - \frac{1}{42}\eta_1^2 \kappa_A \sin \theta_A \quad (29)$$

$$P_{x3} = x_A + \frac{3}{7}\eta_1 \cos \theta_A - \frac{1}{14}\eta_1^2 \kappa_A \sin \theta_A - \frac{1}{210}\eta_1^3 \dot{\kappa}_A \sin \theta_A \quad (30)$$

$$P_{x4} = x_B - \frac{3}{7}\eta_2 \cos \theta_B - \frac{1}{14}\eta_2^2 \kappa_B \sin \theta_B + \frac{1}{210}\eta_2^3 \dot{\kappa}_B \sin \theta_B \quad (31)$$

$$P_{x5} = x_B - \frac{2}{7}\eta_2 \cos \theta_B - \frac{1}{42}\eta_2^2 \kappa_B \sin \theta_B \quad (32)$$

$$P_{x6} = x_B - \frac{1}{7}\eta_2 \cos \theta_B \quad (33)$$

$$P_{x7} = x_B \quad (34)$$

$$P_{y0} = y_A \quad (35)$$

$$P_{y1} = y_A + \frac{1}{7}\eta_1 \sin \theta_A \quad (36)$$

$$P_{y2} = y_A + \frac{2}{7}\eta_1 \sin \theta_A + \frac{1}{42}\eta_1^2 \kappa_A \cos \theta_A \quad (37)$$

$$P_{y3} = y_A + \frac{3}{7}\eta_1 \sin \theta_A + \frac{1}{14}\eta_1^2 \kappa_A \cos \theta_A + \frac{1}{210}\eta_1^3 \dot{\kappa}_A \cos \theta_A \quad (38)$$

$$P_{y4} = y_B - \frac{3}{7}\eta_2 \sin \theta_B + \frac{1}{14}\eta_2^2 \kappa_B \cos \theta_B - \frac{1}{210}\eta_2^3 \dot{\kappa}_B \cos \theta_B \quad (39)$$

$$P_{y5} = y_B - \frac{2}{7}\eta_2 \sin \theta_B + \frac{1}{42}\eta_2^2 \kappa_B \cos \theta_B \quad (40)$$

$$P_{y6} = y_B - \frac{1}{7}\eta_2 \sin \theta_B \quad (41)$$

$$P_{y7} = y_B \quad (42)$$

Via the transformation, we are able to use the Bézier form to simplify the manipulation of the simplified η^3 -spline curve satisfying the boundary conditions by manipulating the control points of the equivalent natural 7th degree Bézier curve, while the convex hull of the control points provides outline of the curve for collision check. In this path design approach, the starting velocity η_1 and the ending velocity η_2 of the forward trajectory (single-directional maneuver) are the two path design parameters.

Our logic of choosing η_1, η_2 is to propose an appropriate eta value to make the trajectory natural and human-like, i.e. a suitable maneuver time and the velocity should be slower for path segments with larger curvature than those with small curvature, verified by a few trial simulations. The initial and final speed needs to be large enough to account for the time optimality, and small enough to meet the constraints without causing large acceleration or angular velocity (change).

Note, let $r(t)$ be the path. $|r'(0)|, |r'(1)|$ are directly proportional to η_1, η_2 parameters. Since the given end curvature κ_A is related to $\frac{r''(0)}{|r'(0)|^2}$. Therefore, too large η_1 will very likely make the path near $t = 0$ straighter (closer to $\overline{P_0P_1}$) while too small η_1 will introduce excessively large curvature at the beginning of the path. Similar reasoning holds for the other end $t = 1$ for the parameter η_2 .

Since η represents the end speed, its value should obey the speed limits set by the vehicle or traffic rules. Most work on continuous-curvature lane change curve design assume the curvature at the ends are zero, which is valid for straight road. From empirical evaluation, symmetric quintic Bézier curve with control points set in a symmetric way is excellent in minimizing lane change time. The travel time T is estimated as $\frac{L}{\eta}$, where L is the path length. Thus, an initial guess of eta we may try is the chord length of $\overline{P_0P_7}$.

In the following driving scenarios we discuss, we use η^3 -spline as single directional maneuver (smooth path without directional change), instead of bidirectional maneuver with forward and backward motions and a sequence of small local maneuvers to fulfill the boundary conditions, which require additional computational effort for joining the different path segments meeting the smoothness constraints.

3 Path Design for curvature-constrained turning

We present three curvature-constrained turning scenarios by using simplified η^3 -spline. All the paths are non-stop, smooth, forward, and single maneuver trajectory solutions. Besides, we normalize the solutions so all of them can be used on every different case. The three scenarios are used to highlight the ease of design of forward curvature-constrained path continuous in configuration (position, heading/tangent), curvature and curvature derivative to satisfy the maximum curvature constraint using 7th degree Bezier curves with two design parameters (the starting velocity and the ending velocity of the forward trajectory).

3.1 Ordinary turn

The first case we want to study is ordinary turn which every vehicle must encounter. For the definition of ordinary turn, it means that the vehicle goes straight at first, turns counterclockwise toward direction θ , and then backs to go straight. Turning the definition into boundary conditions configurations (4) and (5), they become

$$\Omega_A = [x_A, y_A, \theta_A, 0, 0]^T \quad (43)$$

and

$$\Omega_B = [x_B, y_B, \theta_B, 0, 0]^T \quad (44)$$

Without loss of generality, we set $\theta_A = 0^\circ$ and $\theta_B = \theta$. Therefore, the control points equation (27)-(42) can be expressed as

$$P_{x0} = x_A \quad (45)$$

$$P_{x1} = x_A + \frac{1}{7}\eta_1 \quad (46)$$

$$P_{x2} = x_A + \frac{2}{7}\eta_1 \quad (47)$$

$$P_{x3} = x_A + \frac{3}{7}\eta_1 \quad (48)$$

$$P_{x4} = x_B - \frac{3}{7}\eta_2 \cos \theta_B \quad (49)$$

$$P_{x5} = x_B - \frac{2}{7}\eta_2 \cos \theta_B \quad (50)$$

$$P_{x6} = x_B - \frac{1}{7}\eta_2 \cos \theta_B \quad (51)$$

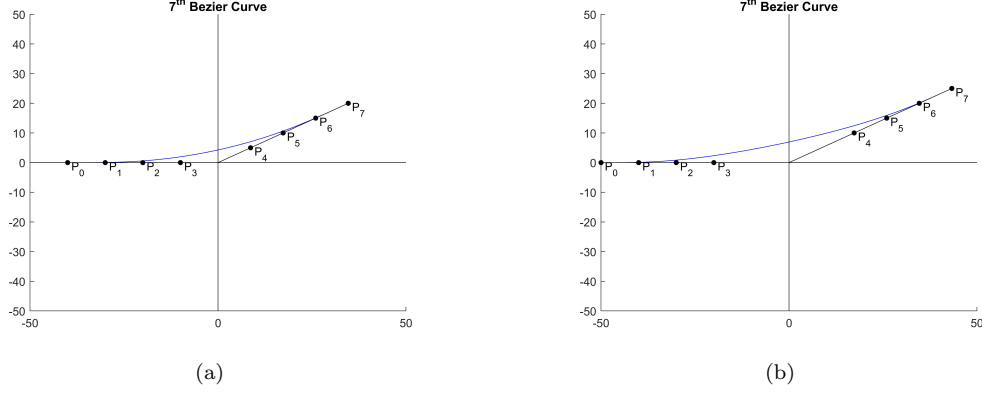


Figure 2: two examples of the design of symmetric 7^{th} order curve in ordinary turn. In each subfigure, the blue curve is the path of Bézier curve and the black points are the control points. (a) is the case with smaller distance between P_3 and P_4 while larger in (b).

$$P_{x7} = x_B \quad (52)$$

$$P_{y0} = y_A \quad (53)$$

$$P_{y1} = y_A \quad (54)$$

$$P_{y2} = y_A \quad (55)$$

$$P_{y3} = y_A \quad (56)$$

$$P_{y4} = y_B - \frac{3}{7}\eta_2 \sin \theta_B \quad (57)$$

$$P_{y5} = y_B - \frac{2}{7}\eta_2 \sin \theta_B \quad (58)$$

$$P_{y6} = y_B - \frac{1}{7}\eta_2 \sin \theta_B \quad (59)$$

$$P_{y7} = y_B \quad (60)$$

Observe the results above, we can find that if $\eta_1 = \eta_2 = \eta$, except P_3 and P_4 , all distances between P_i and P_{i+1} are the same. Therefore, the curve is symmetric with respect to the line that passes through the midpoint of P_i and P_{7-i} , for $i = 0, 1, 2, 3$, like FIGURE 2a and 2b. Moreover, it is reasonable to figure out the vehicle behaviors, such as velocity, curvature, and derivative of curvature, would be symmetric with respect to half of the time, that is $t = 0.5$. With this property, it is ideal for us to constrain the maximum curvature happens at $t = 0.5$.

Given η and θ , the only variables are the end points locations which change the distance between P_3 and P_4 . From FIGURE 2a, we can imagine that the closer P_3 and P_4 are, the more curved the path is at the midpoint. On the other hand, the farther P_3 and P_4 are, the flatter the path is at the midpoint, like FIGURE 2b. That is, the path has maximum curvature closer to $t = 0.5$ when P_3 and P_4 are closer. We find that the maximum curvature will happen at $t = 0.5$ if P_3 and P_4 are the same point. The following is the induction.

Without loss of generality, we set $P_3 = P_4 = (0, 0)$. Given η and θ , from the equation of P_3 and P_4 , (48), (49), (56) and (57) become

$$P_{x3} = x_A + \frac{3}{7}\eta = 0$$

$$P_{x4} = x_B - \frac{3}{7}\eta \cos \theta = 0$$

$$P_{y3} = y_A = 0$$

$$P_{y4} = y_B - \frac{3}{7}\eta \sin \theta = 0,$$

we can get

$$x_A = -\frac{3}{7}\eta = -3A$$

$$x_B = \frac{3}{7}\eta \cos \theta = 3A \cos \theta$$

$$y_A = 0$$

$$y_B = \frac{3}{7}\eta \sin \theta = 3A \sin \theta,$$

where $A = \frac{\eta}{7}$ for simplification. Consequently, the control points equations (45)-(60) become

$$P_{x0} = -3A \quad (61)$$

$$P_{x1} = -2A \quad (62)$$

$$P_{x2} = -A \quad (63)$$

$$P_{x3} = 0 \quad (64)$$

$$P_{x4} = 0 \quad (65)$$

$$P_{x5} = A \cos \theta \quad (66)$$

$$P_{x6} = 2A \cos \theta \quad (67)$$

$$P_{x7} = 3A \cos \theta \quad (68)$$

$$P_{y0} = 0 \quad (69)$$

$$P_{y1} = 0 \quad (70)$$

$$P_{y2} = 0 \quad (71)$$

$$P_{y3} = 0 \quad (72)$$

$$P_{y4} = 0 \quad (73)$$

$$P_{y5} = A \sin \theta \quad (74)$$

$$P_{y6} = 2A \sin \theta \quad (75)$$

$$P_{y7} = 3A \sin \theta \quad (76)$$

With these defined control points, we can rewrite the path equation (26) into

$$\begin{aligned} B_x(t) = & -3A(1-t)^7 - 14At(1-t)^6 - 21At^2(1-t)^5 \\ & + 0 + 0 + 21A \cos \theta t^5(1-t)^2 \\ & + 14A \cos \theta t^6(1-t) + 3A \cos \theta t^7 \end{aligned} \quad (77)$$

and

$$\begin{aligned} B_y(t) = & 0 + 0 + 0 + 0 + 0 + 21A \sin \theta t^5(1-t)^2 \\ & + 14A \sin \theta t^6(1-t) + 3A \sin \theta t^7 \end{aligned} \quad (78)$$

which respectively represent the x part and y part of curve. The two parts first order derivative of the curve are

$$\begin{aligned} \dot{B}_x(t) = & 7A[(1-t)^6 + 6t(1-t)^5 + 15t^2(1-t)^4 \\ & + 15 \cos \theta t^4(1-t)^2 + 6 \cos \theta t^5(1-t) \\ & + \cos \theta t^6] \end{aligned} \quad (79)$$

and

$$\dot{B}_y(t) = 7A \sin \theta [15t^4(1-t)^2 + 6t^5(1-t) + t^6] \quad (80)$$

The two parts of the second derivative of the curve are

$$\ddot{B}_x(t) = 420A[-t^2(1-t)^3 + t^3(1-t)^2 \cos \theta] \quad (81)$$

and

$$\ddot{B}_y(t) = 420A \sin \theta t^3(1-t)^2 \quad (82)$$

Then we can write the curvature equation as

$$\kappa = \frac{\dot{B}_x \ddot{B}_y(t) - \ddot{B}_x(t) \dot{B}_y(t)}{(\dot{B}_x(t))^2 + (\dot{B}_y(t))^2} = \frac{num}{den}. \quad (83)$$

It is obvious that the equation of the derivative of curvature is too complex to analyze. Consequently, we will show that the local maximum of num and local minimum of den both occur at $t = 0.5$.

The numerator of the curvature equation, num , is

$$\begin{aligned} num = & 2940A^2 \sin \theta [t^3(1-t)^8 + 6t^4(1-t)^7 \\ & + 15t^5(1-t)^6 + 15t^6(1-t)^5 + 6t^7(1-t)^4 \\ & + t^8(1-t)^3]. \end{aligned} \quad (84)$$

Let $N(t)$ be

$$\begin{aligned} N(t) = & t^3(1-t)^8 + 6t^4(1-t)^7 + 15t^5(1-t)^6 \\ & + 15t^6(1-t)^5 + 6t^7(1-t)^4 + t^8(1-t)^3. \end{aligned} \quad (85)$$

The derivative of $N(t)$ is

$$\begin{aligned} \dot{N}(t) = & 3t^2(1-t)^8 + 16t^3(1-t)^7 + 33t^4(1-t)^6 \\ & - 33t^6(1-t)^4 - 16t^7(1-t)^3 - 3t^8(1-t)^2. \end{aligned} \quad (86)$$

From (86), we can find the extreme value of the numerator of curvature by finding the roots of $\dot{N}(t)$ which are

$$t = 0, 0, 0, 1, 1, \frac{1}{2}, \frac{1}{10}[5 \pm \sqrt{5(9 \pm 2i\sqrt{26})}].$$

Now we know there is a local extreme value at $t=0.5$. Next, we want to show that the local extreme value is local maximum. Rewrite (86) as

$$\begin{aligned} \dot{N}(t) = & 3[t^2(1-t)^8 - t^8(1-t)^2] \\ & + 16[t^3(1-t)^7 - t^7(1-t)^3] \\ & + 33[t^4(1-t)^6 - t^6(1-t)^4]. \end{aligned} \quad (87)$$

when

$$\begin{aligned} 0 & < t < 0.5, \\ 0.5 & < (1-t) < 1. \end{aligned}$$

Thus, for

$$\begin{aligned} \alpha & < \beta, \\ t^\alpha(1-t)^\beta & > t^\beta(1-t)^\alpha \end{aligned}$$

Since all the three terms in $\dot{N}(t)$ conform the condition $\alpha < \beta$, $\dot{N}(t) > 0$ for $0 < t < 0.5$. $\dot{N}(t) < 0$ for $0.5 < t < 1$, vice and versa. For the conditions above, $N(t)$ has an extreme value at $t = 0.5$ and concaves upward. As a result, $N(t)$ has a local maximum value at $t = 0.5$.

As for the denominator of curvature equation, *den*, is

$$den = (\dot{B}_x(t)^2 + \dot{B}_y(t)^2)^{\frac{3}{2}}. \quad (88)$$

To find the extreme value of *den*, It is equal to calculate the derivative of $\dot{B}_x(t)^2 + \dot{B}_y(t)^2$. Let us define $D(t)$ as

$$D(t) = \dot{B}_x(t)^2 + \dot{B}_y(t)^2. \quad (89)$$

The derivative of $D(t)$ is

$$\begin{aligned} \dot{D}(t) = & 2\dot{B}_x(t)\ddot{B}_x(t) + 2\dot{B}_y(t)\ddot{B}_y(t) \\ = & 5880A^2[t^2(1-t)^9 - 6t^3(1-t)^8 \\ & - 15t^4(1-t)^7 - 15\cos\theta t^6(1-t)^5 \\ & - 6\cos\theta t^7(1-t)^4 - \cos\theta t^8(1-t)^3 \\ & + \cos\theta t^3(1-t)^8 + 6\cos\theta t^4(1-t)^7 \\ & + 15\cos\theta t^5(1-t)^6 + 15t^7(1-t)^4 \\ & + 6t^8(1-t)^3 + t^9(1-t)^2]. \end{aligned} \quad (90)$$

Rewrite it as the same form in $\dot{N}(t)$, it becomes:

$$\begin{aligned} \dot{D}(t) = & 5880A^2\{[-t^2(1-t)^9 + t^9(1-t)^2] \\ & + 6[-t^3(1-t)^8 + t^8(1-t)^3] \\ & + 15[-t^4(1-t)^7 + t^7(1-t)^4] \\ & + 15\cos\theta[-t^6(1-t)^5 + t^5(1-t)^6] \\ & + 6\cos\theta[-t^7(1-t)^4 + t^4(1-t)^7] \\ & + \cos\theta[-t^8(1-t)^3 + t^3(1-t)^8]\}. \end{aligned} \quad (91)$$

So, when $t = 0.5$,

$$\begin{aligned} \dot{D}(0.5) = & 5880A^2\{[-0.5^11 + 0.5^11] + 6[-0.5^11 + 0.5^11] \\ & + 15[-0.5^11 + 0.5^11] + 15\cos\theta[-0.5^11 + 0.5^11] \\ & + 6\cos\theta[-0.5^11 + 0.5^11] \\ & + \cos\theta[-0.5^11 + 0.5^11]\} = 0. \end{aligned}$$

Therefore, $D(t)$ has an extreme value at $t = 0.5$. We can find that the first three terms of $\dot{D}(t)$ confirm the condition

$$\alpha < \beta.$$

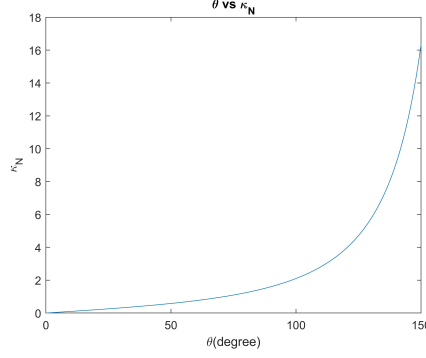


Figure 3: the relation between κ_N and θ

Consequently, the first three terms are negative when $0 < t < 0.5$. However, the last three terms, which contain $\cos \theta$ respectively, don't follow the form. As a result, we have to find whether the sum of the first three terms and last three terms is nonnegative. Since $\cos \theta < 1$,

$$\begin{aligned}
\dot{D}(0.5) &\leq 5880A^2\{-t^2(1-t)^9 + t^9(1-t)^2\} \\
&\quad + 6[-t^3(1-t)^8 + t^8(1-t)^3] \\
&\quad + 15[-t^4(1-t)^7 + t^7(1-t)^4] \\
&\quad + 15[-t^6(1-t)^5 + t^5(1-t)^6] \\
&\quad + 6[-t^7(1-t)^4 + t^4(1-t)^7] \\
&\quad + [-t^8(1-t)^3 + t^3(1-t)^8] \\
&= 5880A^2\{[t^2(1-t)^2((1-t)^6 + t^6)(2t-1)] \\
&\quad + 6[t^3(1-t)^3((1-t)^4 + t^4)(2t-1)] \\
&\quad + 15[t^4(1-t)^4((1-t)^2 + t^2)(2t-1)]\}.
\end{aligned}$$

Only the term $(2t-1)$ can decide $\dot{D}(t)$ is positive or not as the other terms are all positive. The term $(2t-1)$ is negative when $0 < t < 0.5$, so $\dot{D}(t) < 0$ whatever the value θ is. Similarly, when $0.5 < t < 1$, $\dot{D}(t) > 0$. Therefore, $D(t)$ concaves upward and has a local minimum at $t = 0.5$. With the above conditions, we can conclude that the curvature κ has maximum when $t = 0.5$. However, the explicit equation of curvature is too complex because of the term $\sin \theta$ and $\cos \theta$ in $\dot{B}_x(t)$ and $\dot{B}_y(t)$. Fortunately, we know that the numerator of curvature, num, has coefficient A^2 since it is the product of $\dot{B}_x(t)\dot{B}_y(t)$ and $\ddot{B}_x(t)\dot{B}_y(t)$, and the denominator, den, has coefficient A^3 since $\dot{B}_x(t)^2 + \dot{B}_y(t)^2 \propto A^2$. Therefore, the curvature can be expressed as

$$\kappa = \frac{num}{den} \propto \frac{A^2}{A^3} = \frac{1}{A}.$$

For designing path, we define normalized curvature κ_N as

$$\kappa_N = A\kappa \quad (92)$$

We can calculate the relation between κ_N and θ , and multiply A to get true κ . The result is shown in FIGURE 3.

Now, we give an example of our method by setting $A = 10$ and $\theta = 20^\circ$. FIGURE 4 shows the result, including path outline and curvature profile. We can see that the curvature has its maximum value at $t = 0.5$. In FIGURE 3, we can know when $\theta = 20^\circ$, $\kappa_N = 0.2029$. Divide this value by A , and we can get $\kappa = 0.02029$ which is the maximum value of curvature in FIGURE 4.

3.2 Lane change on straight road for 7th order curve

Another case vehicle must encounter is lane change. Lane-change trajectory is a generic turn for vehicle maneuver. For the definition of lane change on straight road, it means that the vehicle goes straight at first, turns to another lane, and then goes straight with the original direction. The boundary conditions configurations (4) and (5) become

$$\Omega_A = [x_A, y_A, \theta, 0, 0]^T \quad (93)$$

and

$$\Omega_B = [x_B, y_B, \theta, 0, 0]^T \quad (94)$$

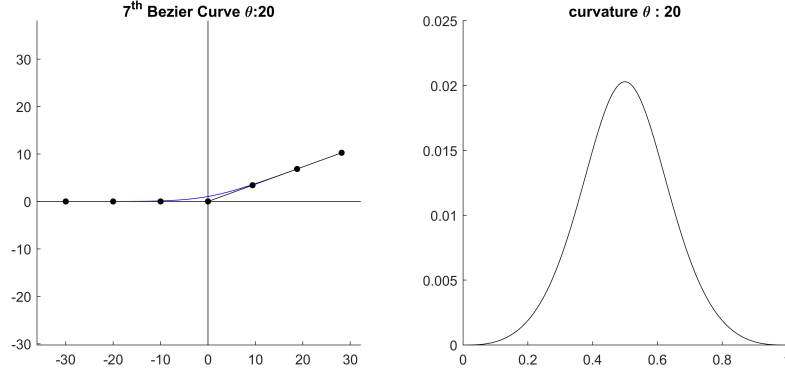


Figure 4: an example path of our method applied in the case of ordinary turn with symmetric curvature. In the left subfigure, the blue curve is the path of Bézier curve and the black points are the control points.

Without loss of generality, we set $\theta = 0^\circ$. Therefore, the control points equation (27)-(42) can be expressed as

$$P_{x0} = x_A \quad (95)$$

$$P_{x1} = x_A + \frac{1}{7}\eta_1 \quad (96)$$

$$P_{x2} = x_A + \frac{2}{7}\eta_1 \quad (97)$$

$$P_{x3} = x_A + \frac{3}{7}\eta_1 \quad (98)$$

$$P_{x4} = x_B - \frac{3}{7}\eta_2 \quad (99)$$

$$P_{x5} = x_B - \frac{2}{7}\eta_2 \quad (100)$$

$$P_{x6} = x_B - \frac{1}{7}\eta_2 \quad (101)$$

$$P_{x7} = x_B \quad (102)$$

$$P_{y0} = y_A \quad (103)$$

$$P_{y1} = y_A \quad (104)$$

$$P_{y2} = y_A \quad (105)$$

$$P_{y3} = y_A \quad (106)$$

$$P_{y4} = y_B \quad (107)$$

$$P_{y5} = y_B \quad (108)$$

$$P_{y6} = y_B \quad (109)$$

$$P_{y7} = y_B \quad (110)$$

FIGURE 5 are examples of this case with control points we show above.

From FIGURE 5a, the vehicle starts from P_0 , turns left, turns right when it is close to the near lane, and then goes straight after the direction of its head backs to 0° . The vehicle behavior is symmetric if $\eta_1 = \eta_2 = \eta$ and therefore the initial and final speed will be the same. However, since the direction of vehicle must change 1 time, the maximum of curvature can't occur at $t = 0.5$.

Similar to the case of ordinary turn, fixed the offset of y coordinate, y_B , the distance between P_3 and P_4 determines when the maximum curvature occurs. It is thinkable that the time that the maximum curvature occurs is close to $t = 0$ if the distance is too far. On the other hand, if the distance is negative, that is, P_4 is at the left-hand side of P_3 , the maximum curvature will occur closer to $t = 0.5$, like what shows in FIGURE 5b. Nonetheless, the path will be too curved as we can see in FIGURE 5b. After some simulations, we decide to let the x coordinate of P_3 and P_4 be the same to make the behavior of vehicle more ideal.

Next, what we are interested in is how the value of η affects the path with given y offset. Without loss of generality, we set $y_A = 0$ and $P_{x3} = P_{x4} = 0$. To reduce the degree of freedom, we set

$$\frac{1}{7}\eta = ry_B = rB \quad (111)$$

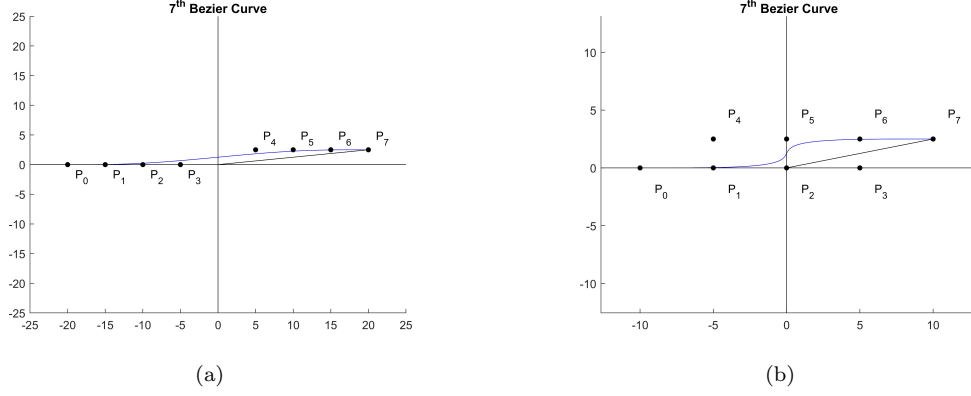


Figure 5: two examples of the design of 7^{th} order curve in lane change on straight road. In each subfigure, the blue curve is the path of Bézier curve and the black points are the control points. (a) is the case with non-overlapped segment along the x-axis while overlapped in (b).

where $B = y_B$ for simplicity and r is a constant. The equations of control points would become

$$P_{x0} = -3rB \quad (112)$$

$$P_{x1} = -2rB \quad (113)$$

$$P_{x2} = -rB \quad (114)$$

$$P_{x3} = 0 \quad (115)$$

$$P_{x4} = 0 \quad (116)$$

$$P_{x5} = rB \quad (117)$$

$$P_{x6} = 2rB \quad (118)$$

$$P_{x7} = 3rB \quad (119)$$

$$P_{y0} = 0 \quad (120)$$

$$P_{y1} = 0 \quad (121)$$

$$P_{y2} = 0 \quad (122)$$

$$P_{y3} = 0 \quad (123)$$

$$P_{y4} = B \quad (124)$$

$$P_{y5} = B \quad (125)$$

$$P_{y6} = B \quad (126)$$

$$P_{y7} = B \quad (127)$$

The x part and y part of path equation from (26) become

$$\begin{aligned} B_x(t) = & -3rB(1-t)^7 - 14rBt(1-t)^6 \\ & - 21rBt^2(1-t)^5 + 0 \\ & + 0 + 21rBt^5(1-t)^2 \\ & + 14rBt^6(1-t) + 3rBt^7 \end{aligned} \quad (128)$$

and

$$\begin{aligned} B_y(t) = & 0 + 0 + 0 + 0 + 35Bt^4(1-t)^3 \\ & + 21Bt^5(1-t)^2 + 7Bt^6(1-t) + Bt^7. \end{aligned} \quad (129)$$

The two parts first order derivative of the curve are

$$\begin{aligned} \dot{B}_x(t) = & 7rB[(1-t)^6 + 6t(1-t)^5 + 15t^2(1-t)^4 \\ & + 15t^4(1-t)^2 + 6t^5(1-t) + t^6] \end{aligned} \quad (130)$$

and

$$\dot{B}_y(t) = 140Bt^3(1-t)^3. \quad (131)$$

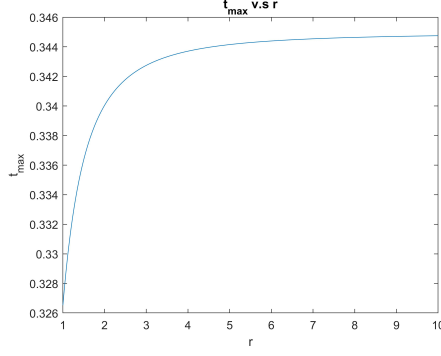


Figure 6: the time that the maximum curvature happens with respect to r

The two parts of the second derivative of the curve are

$$\ddot{B}_x(t) = 420rB[-t^2(1-t)^3 + t^3(1-t)^2] \quad (132)$$

and

$$\ddot{B}_y(t) = -420Bt^2(1-t)^2(2t-1). \quad (133)$$

The third order of derivative of the two parts are

$$\dddot{B}_x(t) = 840rB[-t(1-t)^3 + 3t^2(1-t)^2 - t^3(1-t)] \quad (134)$$

and

$$\dddot{B}_y(t) = -840Bt(1-t)[-5t^2 + 5t - 1]. \quad (135)$$

The curvature of path can be expressed as the same equation of (83),

$$\kappa = \frac{\dot{B}_x(t)\ddot{B}_y(t) - \ddot{B}_x(t)\dot{B}_y(t)}{(\dot{B}_x(t)^2 + \dot{B}_y(t)^2)^{\frac{3}{2}}} = \frac{num}{den}.$$

The numerator is

$$num = -2940rB^2(-1+t)^2t^2(-1+2t), \quad (136)$$

which has local extreme values no matter what the value r is. Nevertheless, r is not the common coefficient of $\dot{B}_x(t)^2 + \dot{B}_y(t)^2$ in the denominator. That means r affects the time that the maximum curvature occurs.

To solve the problem, we use numerical software to calculate the time that the maximum curvature occurs by solving the roots of the derivative of curvature. The derivative of curvature can be expressed as

$$\dot{\kappa} = \left(\frac{num}{den}\right) \quad (137)$$

Where the numerator is

$$\begin{aligned} & (\dot{B}_x(t)\ddot{B}_y(t) - \ddot{B}_x(t)\dot{B}_y(t))(\dot{B}_x(t)^2 + \dot{B}_y(t)^2) \\ & - 3(\dot{B}_x(t)\ddot{B}_y(t) - \ddot{B}_x(t)\dot{B}_y(t))(\dot{B}_x(t)\dot{B}_x(t) \\ & + \dot{B}_y(t)\dot{B}_y(t)). \end{aligned} \quad (138)$$

And the denominator is

$$(\dot{B}_x(t)^2 + \dot{B}_y(t)^2)^{\frac{5}{2}}. \quad (139)$$

Find the roots of the numerator and we can get the time, t_{max} , that the maximum curvature happens. It is noticeable that we only need to find the root that is in $[0, 0.5]$ since the curvature profile is symmetric. The result is shown in FIGURE 6.

Like the case of ordinary turn, the curvature is also proportional to $\frac{1}{B}$ because the numerator, num , which is calculated in (135) has coefficient B^2 and $\dot{B}_x(t)^2 + \dot{B}_y(t)^2$ in the denominator has coefficient B^3 . As a result,

$$\kappa = \frac{num}{den} \propto \frac{B^2}{B^3} = \frac{1}{B},$$

Therefore, normalized curvature, κ_N , in (92) can be used in this case. With t_{max} we calculated in FIGURE 6, we can find the relation of maximum normalized curvature and r , which is shown in FIGURE 7.

Finally, we give an example of this method. We set $B = 5$ and $r = 2$. FIGURE 8 shows the result, including path outline and curvature profile. From FIGURE 6, when $r = 2$, the curvature has its maximum value at $t = 0.34$, consistent with the result in FIGURE 8. In FIGURE 7, we can know when $B = 5$, $\kappa_{N,max} = 0.07215$. Divide this value by B , and we can get $\kappa = 0.01443$ which is the maximum value of curvature in FIGURE 8.

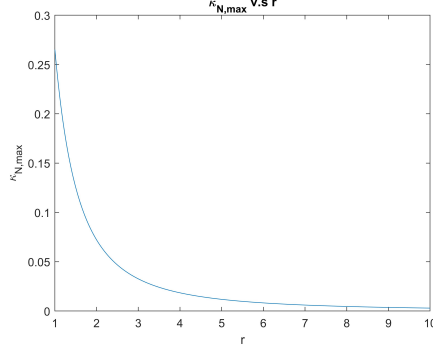


Figure 7: the relation normalized maximum curvature and r

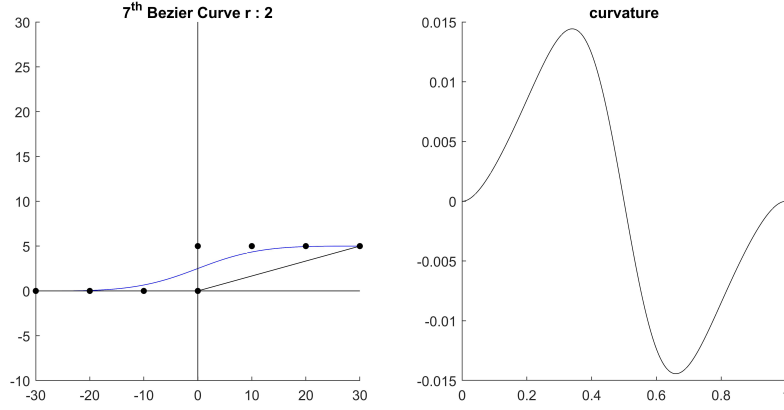


Figure 8: example of our method in the case of lane change on straight road. In the left subfigure, the blue curve is the path of Bézier curve and the black points are the control points.

3.3 Curvature constraint method of lane change in roundabout for 7th order curve

In modern city, roundabout is ubiquitous for its ability to reduce traffic jam. What is common for vehicles in roundabout is lane change when vehicles want to turn into fast speed lane or want to exit roundabout. For the definition of lane change in roundabout, it means that the vehicle drives along a lane, $lane_A$, at first, turns to a new lane, $lane_B$, and then goes along the new lane. The boundary conditions configurations (4) and (5) become

$$\Omega_A = [x_A, y_A, \theta_A, \kappa_A, 0]^T \quad (140)$$

and

$$\Omega_B = [x_B, y_B, \theta_B, \kappa_B, 0]^T \quad (141)$$

The start or terminal state of lane-change in roundabout scenario is located on the lane of roundabout to align with the start or terminal lane tangent, so that the tangent angle, curvature of the start or terminal state in this scenario is determined. Without loss of generality, we set $\theta_A = 0^\circ$ and $\theta_B = \phi$. Thus, as shown in FIGURE 9, ϕ indicates the degree that vehicle passes with respect to the center of roundabout. The positions of end points, (x_A, y_A) and (x_B, y_B) , must be located with respect to the center of roundabout. κ_A and κ_B is the reciprocal of r_A and r_B , the radius of $lane_A$ and $lane_B$. That is, heading at the beginning and end should be tangent to lane in the roundabout. Therefore, we can express (x_A, y_A) and (x_B, y_B) with ϕ , κ_A and κ_B . Without loss of generality, we set $(x_A, y_A) = (0, 0)$. As a result, the center of roundabout is $(0, \frac{1}{\kappa_A})$ and (x_B, y_B) becomes

$$(x_B, y_B) = \left(\frac{1}{\kappa_B} \sin \phi, \frac{1}{\kappa_A} - \frac{1}{\kappa_B} \cos \phi \right). \quad (142)$$

And the configurations of (140) and (141) become

$$\Omega_A = [0, 0, 0^\circ, \kappa_A, 0]^T \quad (143)$$

and

$$\Omega_B = \left[\frac{1}{\kappa_B} \sin \phi, \frac{1}{\kappa_A} - \frac{1}{\kappa_B} \cos \phi, \phi, \kappa_B, 0 \right]^T \quad (144)$$

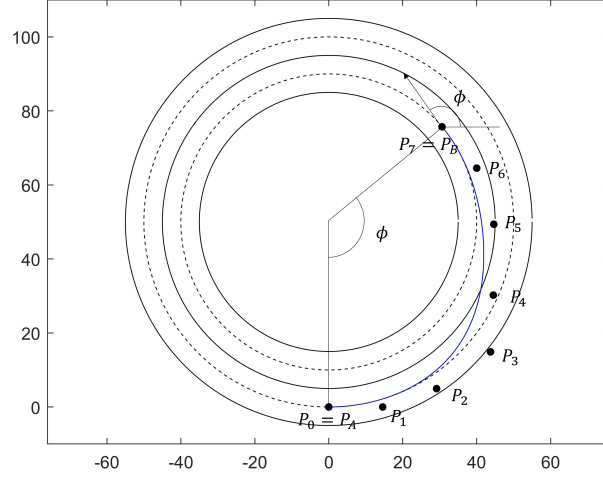


Figure 9: example of 7th order path design in roundabout lane change. The blue curve is the path of Bézier curve and the black points are the control points.

In this case, it is easier to do induction from η^3 -spline aspect. There are lots of variables in the coefficients of $\alpha(t)$ and $\beta(t)$ in (7) and (8) and we mainly focus on how the curvature changes with different end points. Therefore, we define a parameter r' as the ratio of $\frac{r_B}{r_A}$, and set $\eta_1 = \eta_2 = \eta = \frac{h}{\kappa_A}$ to reduce the degrees of freedom, where h is another constant. The coefficients α_i and β_i in (7) and (8) become

$$\alpha_0 = x_A \quad (145)$$

$$\alpha_1 = \frac{h}{\kappa_A} \cos 0^\circ \quad (146)$$

$$\alpha_2 = \frac{1}{2} \frac{h^2}{\kappa_A} \sin 0^\circ \quad (147)$$

$$\alpha_3 = 0 \quad (148)$$

$$\alpha_4 = 35 \frac{r' \sin \phi}{\kappa_A} - 20 \frac{h}{\kappa_A} \cos 0^\circ + 5 \frac{h^2}{\kappa_A} \sin 0^\circ - 15 \frac{h}{\kappa_A} \cos \phi - \frac{5}{2} \frac{h^2}{r' \kappa_A} \sin \phi \quad (149)$$

$$\alpha_5 = -84 \frac{r' \sin \phi}{\kappa_A} + 45 \frac{h}{\kappa_A} \cos 0^\circ - 10 \frac{h^2}{\kappa_A} \sin 0^\circ + 39 \frac{h}{\kappa_A} \cos \phi + 7 \frac{h^2}{r' \kappa_A} \sin \phi \quad (150)$$

$$\alpha_6 = 70 \frac{r' \sin \phi}{\kappa_A} - 36 \frac{h}{\kappa_A} \cos 0^\circ + \frac{15}{2} \frac{h^2}{\kappa_A} \sin 0^\circ - 34 \frac{h}{\kappa_A} \cos \phi - \frac{13}{2} \frac{h^2}{r' \kappa_A} \sin \phi \quad (151)$$

$$\alpha_7 = -20 \frac{r' \sin \phi}{\kappa_A} + 10 \frac{h}{\kappa_A} \cos 0^\circ - 2 \frac{h^2}{\kappa_A} \sin 0^\circ + 10 \frac{h}{\kappa_A} \cos \phi + 2 \frac{h^2}{r' \kappa_A} \sin \phi \quad (152)$$

$$\beta_0 = y_A \quad (153)$$

$$\beta_1 = \frac{h}{\kappa_A} \sin 0^\circ \quad (154)$$

$$\beta_2 = \frac{1}{2} \frac{h^2}{\kappa_A} \cos 0^\circ \quad (155)$$

$$\beta_3 = 0 \quad (156)$$

$$\beta_4 = 35 \frac{1 - r' \cos \phi}{\kappa_A} - 20 \frac{h}{\kappa_A} \sin 0^\circ - 5 \frac{h^2}{\kappa_A} \cos 0^\circ - 15 \frac{h}{\kappa_A} \sin \phi + \frac{5}{2} \frac{h^2}{r' \kappa_A} \cos \phi \quad (157)$$

$$\beta_5 = -84 \frac{1 - r' \cos \phi}{\kappa_A} + 45 \frac{h}{\kappa_A} \sin 0^\circ + 10 \frac{h^2}{\kappa_A} \cos 0^\circ + 39 \frac{h}{\kappa_A} \sin \phi - 7 \frac{h^2}{r' \kappa_A} \cos \phi \quad (158)$$

$$\beta_6 = 70 \frac{1 - r' \cos \phi}{\kappa_A} - 36 \frac{h}{\kappa_A} \sin 0^\circ - \frac{15}{2} \frac{h^2}{\kappa_A} \cos 0^\circ - 34 \frac{h}{\kappa_A} \sin \phi + \frac{13}{2} \frac{h^2}{r' \kappa_A} \cos \phi \quad (159)$$

$$\beta_7 = -20 \frac{1 - r' \cos \phi}{\kappa_A} + 10 \frac{h}{\kappa_A} \sin 0^\circ + 2 \frac{h^2}{\kappa_A} \cos 0^\circ + 10 \frac{h}{\kappa_A} \sin \phi - 2 \frac{h^2}{r' \kappa_A} \cos \phi \quad (160)$$

We can see that except for α_0 and β_0 , the other coefficients have the common coefficient $\frac{1}{\kappa_A}$, and the curvature equation is

$$\kappa = \frac{\dot{\alpha}\ddot{\beta} - \ddot{\alpha}\dot{\beta}}{(\dot{\alpha}^2 + \dot{\beta}^2)^{\frac{3}{2}}}, \quad (161)$$

where

$$\dot{\alpha}(t) = \alpha_1 + 2\alpha_2 t + 3\alpha_3 t^2 + 4\alpha_4 t^3 + 5\alpha_5 t^4 + 6\alpha_6 t^5 + 7\alpha_7 t^6, \quad (162)$$

$$\ddot{\alpha}(t) = 2\alpha_2 + 6\alpha_3 t + 12\alpha_4 t^2 + 20\alpha_5 t^3 + 30\alpha_6 t^4 + 42\alpha_7 t^5, \quad (163)$$

$$\dot{\beta}(t) = \beta_1 + 2\beta_2 t + 3\beta_3 t^2 + 4\beta_4 t^3 + 5\beta_5 t^4 + 6\beta_6 t^5 + 7\beta_7 t^6, \quad (164)$$

and

$$\ddot{\beta}(t) = 2\beta_2 + 6\beta_3 t + 12\beta_4 t^2 + 20\beta_5 t^3 + 30\beta_6 t^4 + 42\beta_7 t^5 \quad (165)$$

Consequently, the curvature equation is

$$\frac{\dot{\alpha}\ddot{\beta} - \ddot{\alpha}\dot{\beta}}{(\dot{\alpha}^2 + \dot{\beta}^2)^{\frac{3}{2}}} = \frac{\frac{1}{\kappa_A^2} \times num}{\frac{1}{\kappa_A^3} \times den} = \kappa_A \frac{num}{den}, \quad (166)$$

where *num* and *den* are polynomials without κ_A . That is, the value of κ_A is not important since it is just a scaling coefficient. What important is the value of r' which can directly change the profile of curvature.

The derivative of $\frac{num}{den}$ determines the local extreme points of curvature. By finding the roots of $(\frac{num}{den})'$, we can get the time, t_{max} , that the maximum curvature, κ_{max} , happens and get the ratio between κ_{max} and κ_A . However, the curve equation is too complex to calculate. Therefore, we turn into numerical simulation based on the change of r' .

By experimental simulation, we choose $\eta = \frac{1}{2}(\frac{1}{\kappa_A} + \frac{1}{\kappa_B})\phi = \frac{1}{2}(\frac{r'+1}{\kappa_A})\phi$ which is close to the total length the path moves. That is,

$$h = \frac{1}{2}(r' + 1)\phi. \quad (167)$$

There are two kinds of curve in the case of roundabout lane change which are shown in the FIGURE 10. The main difference between these two curves is that the direction changes in the left figure, however it doesn't in the right figure. We think the path in the right figure is more ideal in roundabout lane change. The main variable that controls this scenario is ϕ . Therefore, we find the minimum degree, ϕ_{min} , that lets the direction of path doesn't change and the result is shown in FIGURE 11.

The derivative of curvature in this case can be expressed as

$$\frac{(\dot{\alpha}\ddot{\beta} - \ddot{\alpha}\dot{\beta})(\dot{\alpha}^2 + \dot{\beta}^2) - 3(\dot{\alpha}\ddot{\beta} - \ddot{\alpha}\dot{\beta})(\dot{\alpha}\ddot{\alpha} + \dot{\beta}\ddot{\beta})}{(\dot{\alpha}^2 + \dot{\beta}^2)^{\frac{5}{2}}} \quad (168)$$

With ϕ_{min} , we can calculate the relation between t_{max} and k numerically by solving the roots of the numerator in (168), and the outcome is shown as FIGURE 12. For $\phi > \phi_{min}$ the maximum curvature would be smaller. Consequently, the largest curvature of the path without changing direction is at $\phi = \phi_{min}$. It is reasonable since with larger ϕ , the vehicle would go through longer path, and the path is of course smoother.

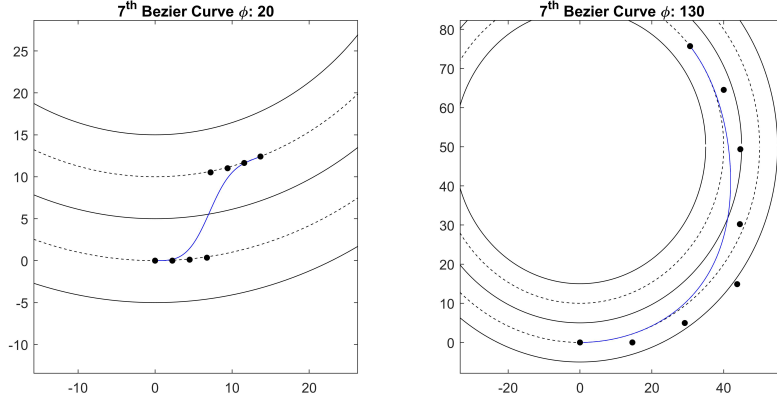


Figure 10: two kinds of 7th curve design for roundabout lane change. In each subfigure, the blue curve is the path of Bézier curve and the black points are the control points. The left one with smaller deflection angle (20°) has more curved path while the right one with the larger deflection angle (130°) does not.

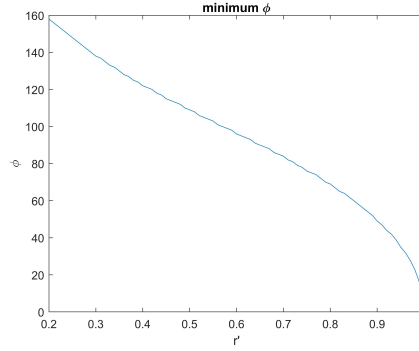


Figure 11: the relation between ϕ_{min} and r'

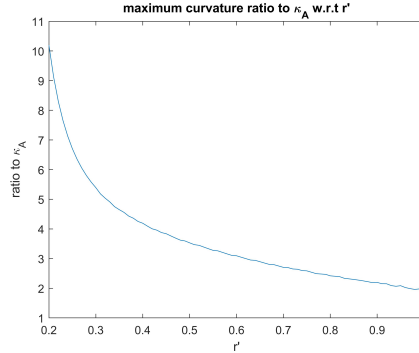


Figure 12: the relation between the ratio of κ_{max} and κ_A and k

The following is the example. In this example, we choose $r' = 0.8$. According to FIGURE 11, we get $\phi_{min, r'=0.8} = 69$ and based on FIGURE 12, we have $\frac{\kappa_{max}}{\kappa_A} = 2.4190$. In FIGURE 13, $\kappa_A = \frac{1}{50}$. The maximum curvature is $2.4190\kappa_A = 2.4190 \cdot \frac{1}{50} = 0.484$ which is marked in FIGURE 13.

4 Conclusion

Since simplified η^3 -spline is a complex curve with high degree of freedom, the curvature equation is hard to analyze. In this paper, we seek a forward(uni-directional) trajectory based on simplified η^3 -spline, which has G^3 smoothness and flexibility to take the comfort (small curvature derivative) into account and reduce the degree of freedom via the transformation to Bézier form with two free parameters restricted in a box constraint. We also illustrate the simplicity and flexibility of the efficient convex path parameters computation procedure by leveraging

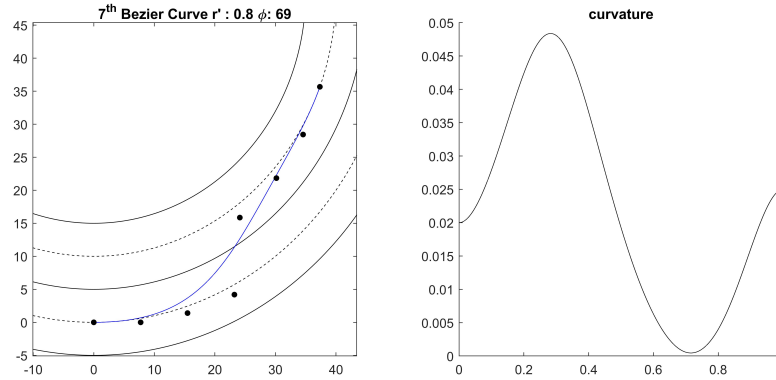


Figure 13: example of our method in the case of roundabout lane change. In the left subfigure, the blue curve is the path of Bézier curve and the black points are the control points.

the nice geometric properties of Bézier curves via three practical curvature-constrained turning maneuver cases that admits simplified η^3 -spline trajectory solutions. In the simplest case, ordinary turn, it has explicit solution. However, the other two cases, lane change on straight road and roundabout lane change may have to turn into numerical calculation instead of explicit solution. With our method, flexibility for design of turning maneuvers with physical constraints such as the maximum curvature and steering angle constraint is considered in this paper. Nonetheless, there are still many cases we have not discussed yet, like entering roundabout and U turn. Therefore, our future work is to keep finding the method to design path with more different cases. Another work in our to-do list is to implement our method on path searching algorithms to compare the searching time with and without our method.

References

- [1] D. Korzeniowski and G. Ślaski. Method of planning a reference trajectory of a single lane change manoeuver with Bézier curve. IOP Conference Series: Materials Science and Engineering. 2016;148:012012.
- [2] Zvi Shiller and Satish Sunda. Emergency Lane-Change Maneuvers of Autonomous Vehicles. ASME Jpurnal of Dynamic Systems, Measurement and Control. 1998 March;120(1):37-44.
- [3] Ho, Man Lung, Ping T. Chan, and A. B. Rad. Lane change algorithm for autonomous vehicles via virtual curvature method. Journal of Advanced Transportation 2009;43(1):47-70.
- [4] J. Pérez, J. Godoy, J. Villagrà and E. Onieva. Trajectory generator for autonomous vehicles in urban environments. IEEE International Conference on Robotics and Automation. 2013;409-414
- [5] Ray Lattarulo, Leonardo González, Enrique Martí, José Matute, Mauricio Marcano, and Joshue Pérez. Urban Motion Planning Framework Based on N-Bézier Curves Considering Comfort and Safety. Journal of Advanced Transportation. 2018 Jul 15;2018:1-13.
- [6] S. Nayak and M. W. Otte. Bidirectional Sampling-Based Motion Planning Without Two-Point Boundary Value Solution. IEEE Transactions on Robotics. 2022;1-19.
- [7] Haoyue Liu,,Xuebo, Zhang, Jian-Wen, RunhuaWang, and XiangChen. Goal-biased Bidirectional RRT based on Curve-smoothing. IFAC-PapersOnLine. 2019;52(24):255-260.
- [8] Neto, Armando A., Douglas G. Macharet, and Mario FM Campos. Feasible RRT-based path planning using seventh order Bézier curves. IEEE/RSJ International Conference on Intelligent Robots and Systems. 2010;1445-1450.
- [9] Aurelio Piazzzi, Corrado Guarino Lo Bianco and Massimo Romano. Smooth Path Generation for Wheeled Mobile Robots Using η^3 -Splines. Motion Control. London, United Kingdom: IntechOpen, 2010 [Online]. Available: <https://www.intechopen.com/chapters/6579> doi: 10.5772/6960
- [10] Ting-Wei Hsu and Jing-Sin Liu. Design of smooth path based on the conversion between η^3 -spline and Bézier curve. American Control Conference (ACC). 2020;3230-3235.
- [11] Ting-Wei Hsu and Jing-Sing Liu. Convex hull determination method for generating Bézier curve followed by Trailer-tractor System. Automation. 2020 Nov. Available from: <https://docplayer.net/218105865-Convex-hull-determination-method-for-generating-bezier-curve-followed-by-trailer-tractor-system.html>.
- [12] Ji-wung Choi, Renwick E. Curry, and Gabriel Hugh Elkaim. Minimizing the maximum curvature of quadratic Bézier curves with a tetragonal concave polygonal boundary constraint. Computer. Aided Des. 2012;44(4):311-319.

- [13] R. Cimurs, J. Hwang and I. H. Suh. Bézier Curve-Based Smoothing for Path Planner with Curvature Constraint. First IEEE International Conference on Robotic Computing (IRC). 2017;241-248.
- [14] H. Li, Y. Luo and J. Wu. Collision-Free Path Planning for Intelligent Vehicles Based on Bézier Curve. IEEE Access. 2019;7:123334-123340.
- [15] C. H. Wei and J. S. Liu. Hybridizing RRT and variable-length genetic algorithm for smooth path generation. IEEE International Conference on Robotics and Biomimetics 2011;626-632.
- [16] A. Piazzzi, C. Guarino Lo Bianco and M. Romano. η^3 -Splines for the Smooth Path Generation of Wheeled Mobile Robots. IEEE Transactions on Robotics. 2007 Oct;23(5)1089-1095.
- [17] Chen, Cheng and He, Yuqing and Bu, Chunguang and Han, Jianda and Zhang, Xuebo. Quartic Bézier curve based trajectory generation for autonomous vehicles with curvature and velocity constraint. IEEE International Conference on Robotics and Automation. 2014 May;6108-6113.
- [18] Fraichard, T., and Scheuer, A. From Reeds and Shepp's to continuous-curvature paths. IEEE Transactions on Robotics, 2004;20(6):1025-1035.
- [19] Zhang, B., Zhang, J., Liu, Y., Guo, K., and Ding, H. Planning flexible and smooth paths for lane-changing manoeuvres of autonomous vehicles. IET Intelligent Transport Systems. 2021 Feb;15(2):200-212.
- [20] Maekawa, T., Noda, T., Tamura, S., Ozaki, T., and Machida, K. I. Curvature continuous path generation for autonomous vehicle using B-spline curves. Computer-Aided Design. 2010;42(4):350-359.
- [21] Wu, C. S., Chiu, Z. Y., and Liu, J. S. Time-optimal trajectory planning along parametric polynomial lane-change curves with bounded velocity and acceleration: simulations for a unicycle based on numerical integration. Modelling and Simulation in Engineering. 2018 Nov;2018:1-19.
- [22] Yang, K., and Sukkarieh, S. An analytical continuous-curvature path-smoothing algorithm. IEEE Transactions on Robotics, 2010 Jun;26(3):561-568.